# PREDICTION OF WELD SHAPE FACTOR IN FLUX BONDED GAS TUNGSTEN ARC WELDING FOR AISI 1020 STEEL

**Harish Kumar Arya**
AssistantProfessor, Mechanical Engineering,
Sant Longowal Institute of Engineering & Technology, Longowal
Email- arya.iitr@gmail.com
**Deepti Jaiswal**
Assistant Professor, Mechanical & Automation Engineering,
Indira Gandhi Delhi Technical University for Women, Delhi
Email-deeptijaiswal2007@gmail.com
**Robin Singh**
Research Scholar, Mechanical Engineering,
Sant Longowal Institute of Engineering & Technology, Longowal
Email-robinthakur33@gmail.com

## ABSTRACT
GTAW welding has a number of drawbacks, the most significant of which is the limited thickness of material that can be welded in a single pass, resulting in a decreased production rate. Thus, a new welding technique Flux Bonded Gas Tungsten Arc Welding used which limits the drawbacks of the GTAW process. In the present work, GTAW process is carried out on AISI 1020 carbon steel plates of 10mm thickness. The specimens were welded as bead on plate. Shape factor is calculated for FB-GTAW and compared with GTAW process. The microstructures and micro hardness are compared with flux and without flux at different heat inputs. The simulation of FB-GTAW process was done by NASTRAN® software. The shape factor predicted by simulation and compared with experimental shape factor at different heat inputs. Time temperature data was measured by NASTRAN® software and compared with experimental time temperature data. The shape factor decreases by FB-GTAW as compared with GTAW process. The shape factor by FB-GTAW decrease by 29.22%, 19.59% and 31.13% at 120, 140 and 160 A respectively. The Micro-hardness of more than 300HV was measured in FB-GTAW process. The Micro-hardness measured was about 200HV. The Micro-hardness measured with FB-GTAW is more than normal GTAW process. This is because due to high cooling rate the martensite formation takes place in the weld pool by FB-GTAW process. While with normal GTAW process acicular ferrite and pearlite are observed in the weld metal. The FB-GTAW process shows that there was maximum error of 0.395% calculated after comparing simulation and experimental shape factor. The simulation peak temperature was 1387°C, 1300°C and 1250°C at 160 A, 140 A and 120 A respectively. Experimental results were 1350°C, 1280°C and 1235°C at above respective currents.

**KEYWORDS:** FB-GTAW, AISI 1020 steel, bead profile, Micro-structure and Micro-hardness, shape factor, Time- Temperature plot and NASTRAN® software.

## 1. INTRODUCTION
TIG is an arc welding process where the work is continuously heated by an electric arc created between the work piece and the metal electrode supply constantly. One of the most commonly used methods in the industry is tungsten inert gas welding [1]. Argon and helium are mostly used shielding gases. The shielding gases are used to protect the weld pool from

atmospheric contamination. The electrode is connected to the power supply negative terminal. Direct current electrode negative (DCEN) is the most frequently used polarity in GTAW process. It is also known as straight polarity [2]. Flux bonded GTAW is alternative of more used welding process A-GTAW process. These are the welding processes generally used to increase the depth of penetration as achieved by the normal GTAW process. In FB-GTAW process basically, the flux is applied on the plate and a small gap (generally called as flux gap) was made at the centre of the plate [3]. Since the least resistive direction is chosen by the electrons, electrons are channelled only inside the flux gap. The effect is thus generally called insulation effect. The depth of penetration has been increased and bead width has been constricted by with FB-GTAW process as compared with normal GTAW process. it was found that when the number of surface-active elements increases the direction of metal flow changes from outward to inward this was due to change in surface temperature gradient at the periphery of weld pool from negative to positive. Due to this the metal flows in reverse direction from outward to inward (Reverse Marangoni effect) [3]. AISI 1020 carbon steel was used as the base metal. It is used in structural parts, pipelines. It contains carbon content of 0.20% by weight. The silicon dioxide layer was applied on the base metal. Silicon dioxide is an acidic oxide that forms the main component of all the fluxes and provides the viscosity and current carrying capacity required in the molten state of flux. The viscosity and the current carrying capacity of the flux also stay high while the $SiO_2$ content is greater. In addition, with strong weld bead appearance without undercut, slag detachability is improved [4].The finite element modelling of the work is done with the help of NASTRAN software. This approach deals with three instruments such as theoretical, experimental and computational techniques to predict the behaviour of the structure. The solution obtained by the analytical method is accurate and require less time. For irregular parts and shapes that involve very complex mathematical equations, this approach cannot be used. There are several numerical schemes used to estimate the approximate solutions of appropriate tolerance, such as finite difference method, boundary element and volume method, finite strip and volume method and boundary integral methods etc. The finite element approach is the most flexible and commonly used for examining complex engineering [5].G. Ruckert has studied the performance of silica coatings on AISI 304L stainless steel GTAW [6]. Shirish R. Kalaet al. has done modelling using temperature and phase-based material properties on 6 mm mild steel plates [7]. Tseng K.H. & Shiu Y.J. has discussed the effect of thermal stability of powered oxide on joint penetration and metallurgical feature of AISI 4139 steel TIG weldment [8]. Akhilesh Kumar Singh et al. have discussed the techniques to improve weld penetration in TIG welding [9].Kamlesh Kumar has studied the comparison between normal TIG welding and the activated TIG welding on 3 mm thick AISI 304 stainless steel plate. The result shows that the depth of penetration increased in FB-GTAW process as compared to normal GTAW process [10]. Vidyarthy R.S. & Sivateja P. has studied the influence of activating flux tungsten inert gas welding on mechanical and metallurgical properties of the mild steel. Theresults show that the martensite was formed in the weld metal by FB-GTAW process due to high cooling rate [11]. Unni A.K & Vasudevan M. has worked on the creation of the weld pool when welding activated tungsten inert gas (A-TIG) using computational fluid dynamics(CFD). The study shows that the addition of oxygen content changes the temperature coefficient of surface tension from negative to positive gradient that induces inward flow [12].

## 2. MATERIALS AND WORK METHODOLOGY

### 2.1. MATERIALS USED

AISI 1020 is used as the base material to perform experiments and simulation. The materialproperties are given in Table 1. It is widely used in pipeline, machine parts and structural parts. It has carbon percentage by weight of 0.20, manganese 0.30, phosphorus

0.040, sulphur 0.05 and remaining percentage of iron. The size of the material used is 300×130×10 (L×B×T) mm.

Table 1 Chemical properties of AISI 1020

| Carbon | Iron | Manganese | Phosphorus | Sulphur |
|---|---|---|---|---|
| 0.20 % | 99.47 % | 0.30 % | 0.040% | 0.05% |

## 2.2.METHODOLOGY OF EXPERIMENTAL WORK

The methodology of the experimental work is shown in Figure 1. After the selection of material, the process is selected as GTAW. The two types of study are done with flux and without flux. Then the shape factor is calculated by FB-GTAW and GTAW process and compared. The Micro-structure of weld metal is compared for FB-GTAW and GTAW process. The Micro-hardness is compared for FB-GTAW and GTAW process. The bonded flux used is silicon dioxide. The mixture of the flux is prepared by mixing it with acetone and sodium silicate binder. Then it is applied on the base metal with the help of brush or by spray. Then it is allowed to evaporate and a layer of flux is formed on the base metal. The composition of the flux used is given in Table 2.

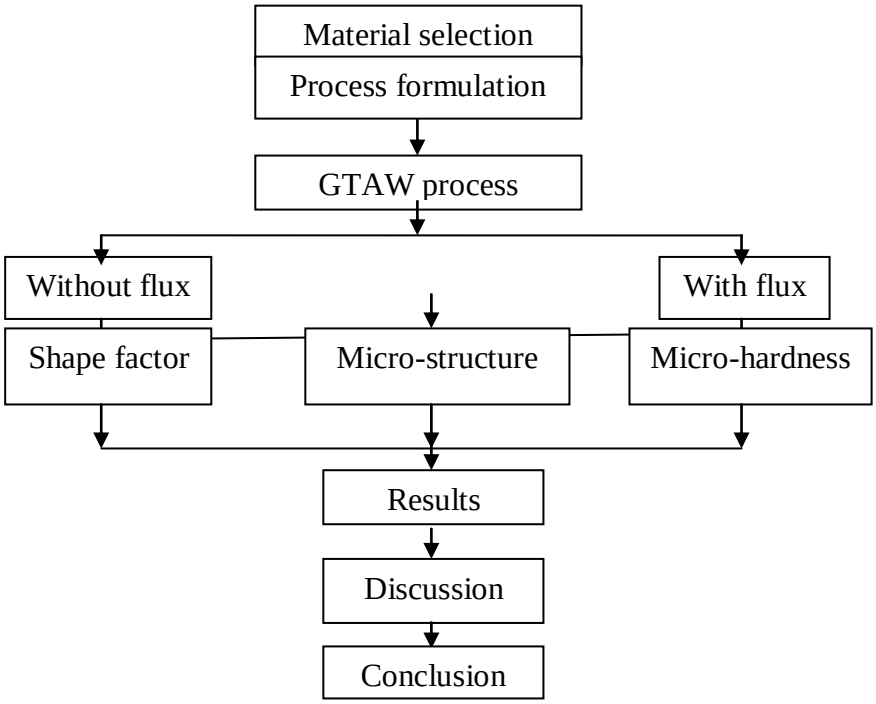


Figure 1.Methodology of experimental work

The bonded flux used is silicon dioxide. The mixture of the flux is prepared by mixing it with acetone and sodium silicate binder. Then it is applied on the base metal with the help of brush or by spray. Then it is allowed to evaporate and a layer of flux is formed on the base metal. The composition of the flux used is given in Table 2.

Table 2 Composition of activated flux used

| Components used | Amount (units) |
|---|---|
| $SiO_2$ activating flux | 1.2 gms |

| | |
|---|---|
| Acetone solvent | 10 ml |
| Sodium silicate binder | 2 drops |

After welding the samples is cut the polishing is done with the help of emery papers of different grades. Then the etching of the polished specimen is done with nital solution. Nital is the mixture of methanol and 2% nitric acid. The etching must be done for 15-20 seconds. The Micro-structure is observed by the optical microscopy by LEICA DMI 50 M microscope. The Micro-hardness is calculated by VICKERS Micro-hardness testing machine at SLIET Longowal Metallurgy lab. In Micro-hardness test the load is applied for 10-20 seconds so that it does not harm in such a way. After removing the load, the impression of square shape is seen. This gives the Micro-hardness of the given metal.

## 3.FINITE ELEMENT FORMULATION

The simulation of the work is done using NASTRAN® software. The MSc Marc do the linear and non-linear engineering simulations smoothly and efficient than any other finite element codes that are existing today. The boundary conditions can be applied within the integrated MSc Marc® setting and either on the geometry of the model or on the entities of finite elements. The MSc Marc software is used for temperature and time-temperature of AISI 1020 low carbon steel by using Gas Tungsten Arc Welding. The heat transfer analysis done in welding to get temperature profile. The temperature profile at various currents are calculated and compared with the experimental time-temperature data.

## 4. RESULTS AND DISCUSSIONS

### 4.1. SHAPE FACTOR CALCULATION

The depth of penetration increases as the heat input increases in GTAW process. But at the same heat input the depth of penetration can be increased by FB-GTAW process. The depth of penetration at 120A was 2.02 mm and bead width were 6.22 mm by GTAW process while at the same current value penetration and bead width was 2.8 mm and 6.1mm respectively. The shape factor at 120A by using flux coating is 2.18 which is less than 3.08 without using flux coating. The depth of penetration and bead width at 140 A was 2.43 mm and 6.54 mm in GTAW while in FB-GTAW the bead width and depth of penetration was 6.51 mm and 3.01 mm respectively. The shape factor at 140 A is 2.163 by FB-GTAW which is less than 2.69 as achieved in GTAW. The depth of penetration and bead width at 160 A was 2.45 and 6.54 mm in GTAW. The depth of penetration and bead width was 3.54 mm and 6.51 mm at 160 A. Shape factor at 160 A is 1.77 by using flux coating which is less than 2.57 as achieved in without using flux coating

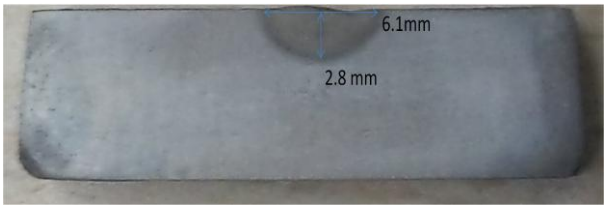


Figure2 Depth of penetration and bead width at 120 A (FB-GTAW)

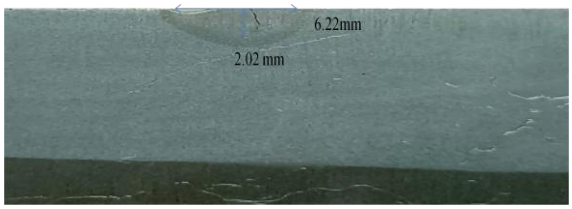


Figure3 Depth of penetration and bead width at 120 A (GTAW)

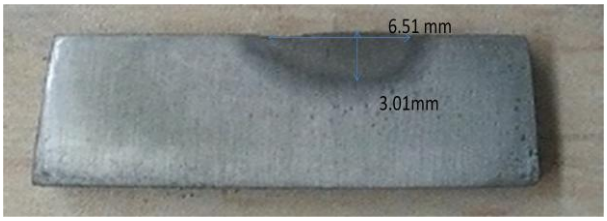


Figure4 Depth of penetration and bead width at 140 A (FB-GTAW)

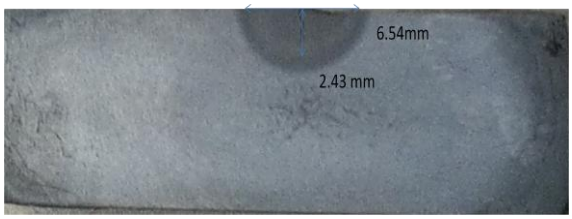


Figure5 Depth of penetration and bead width at 140 A (GTAW)

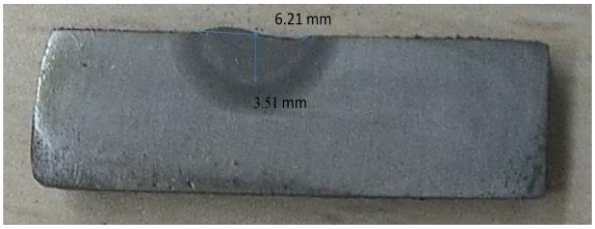


Figure6 Depth of penetration and bead width at 160 A (FB-GTAW)

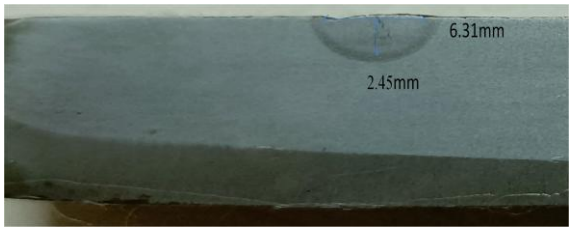


Figure7Depth of penetration and bead width at 160 A (GTAW)

Table 3 Comparison of Shape factor (GTAW and FB-GTAW)

| Current (A) | Voltage (V) | Depth of penetration (mm) | | Bead width (mm) | | Shape factor | |
|---|---|---|---|---|---|---|---|
| | | FB-GTAW | GTAW | FB-GTAW | GTAW | FB-GTAW | GTAW |
| 120 | 12 | 2.8 | 2.02 | 6.1 | 6.22 | 2.18 | 3.08 |
| 140 | 12 | 3.01 | 2.43 | 6.51 | 6.54 | 2.163 | 2.69 |
| 160 | 12 | 3.51 | 2.45 | 6.21 | 6.31 | 1.77 | 2.57 |

**4.2.MICROSTRUCTURE STUDY OF THE WELD ZONE**

At 120A the martensite formation starts due to formation of austenite in the weld metal. This transformation is achieved at high cooling rate. The cooling rate at 120 A is 160.22 °C/s and peak temperature is 1175°C with FB-GTAW process as calculated from Time-Temperature plot.

The cooling rate at 140 A is 138.61 °C/s and peak temperature is 1250°C with Flux Bonded Gas Tungsten Arc Welding. The ferrite content decreases with the increase with increase in welding current. As the welding current decrease the levels of ferrite decreases. In normal GTAW there is formation of acicular ferrite and pearlite in the weld metal.

As the current is increased to 160 A the cooling rate will be lower. This is due to low cooling rate which leads to decrease in the levels of ferrite in the weld metal. The cooling rate at 160 A is 96.67 °C/s and peak temperature is 1350°C as calculated from Time-Temperature plot for FB-GTAW process

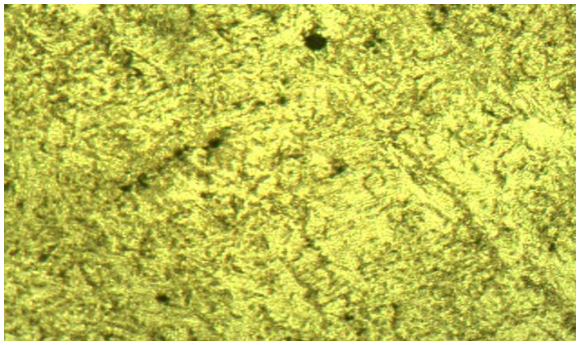

Figure 8 Weld metal microstructure for FB-GTAW at 120 A

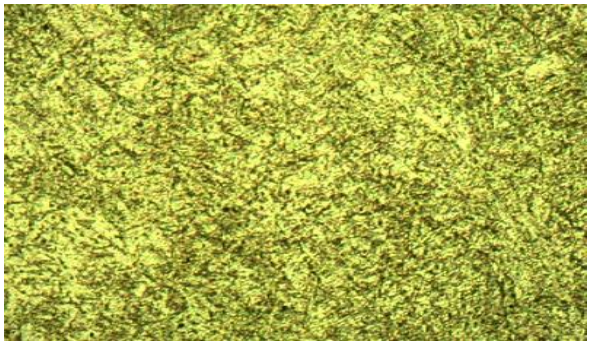

Figure9Weld metal microstructure for GTAW at 120 A

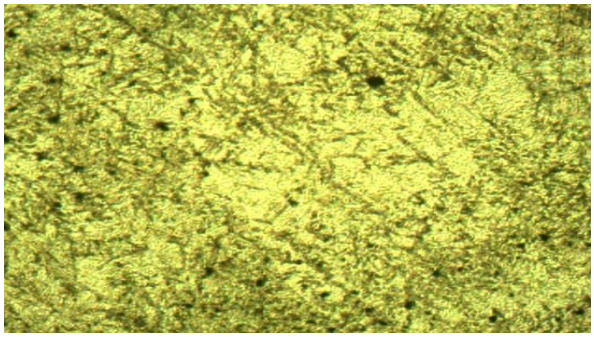

Figure 10 Weld metal microstructure for FB-GTAW at 140 A

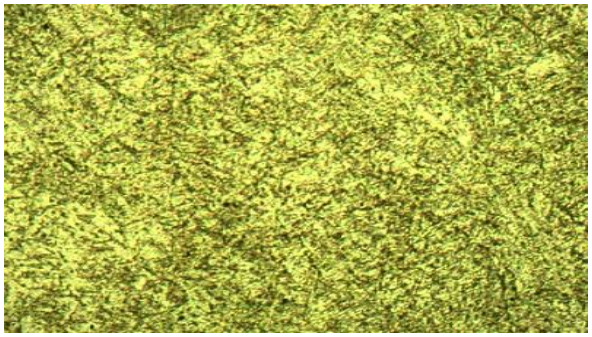

Figure11 Weld metal microstructure for GTAW at 140 A

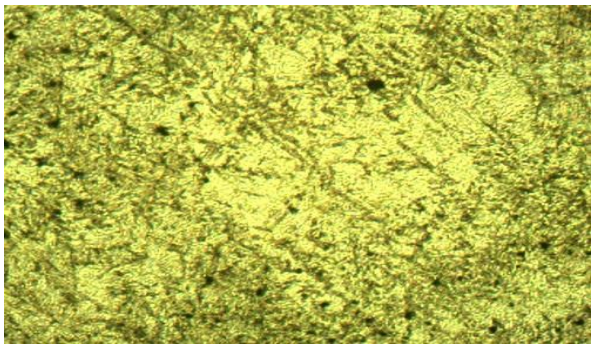

Figure12Weld metal microstructure for FB-GTAW at 160 A

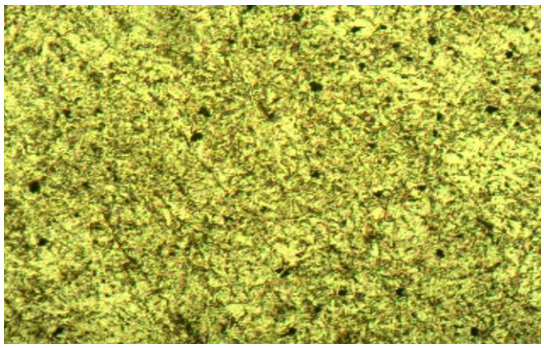

Figure 13 Weld metal microstructure for FB-GTAW at 140 A

### 4.3. MICRO- HARDNESS OBSERVATIONS

#### 4.3.1. MICRO HARDNESS AT 120 AMPERE BY FB-GTAW AND GTAW

The above study shows that in FB-GTAW process martensite forms in the weld pool due to this the hardness of the weld metal has been increased. The micro hardness of 350HV has been recorded at weld centre. In normal GTAW process the hardness in the weld metal was 260 HV which was less than flux bonded GTAW process.

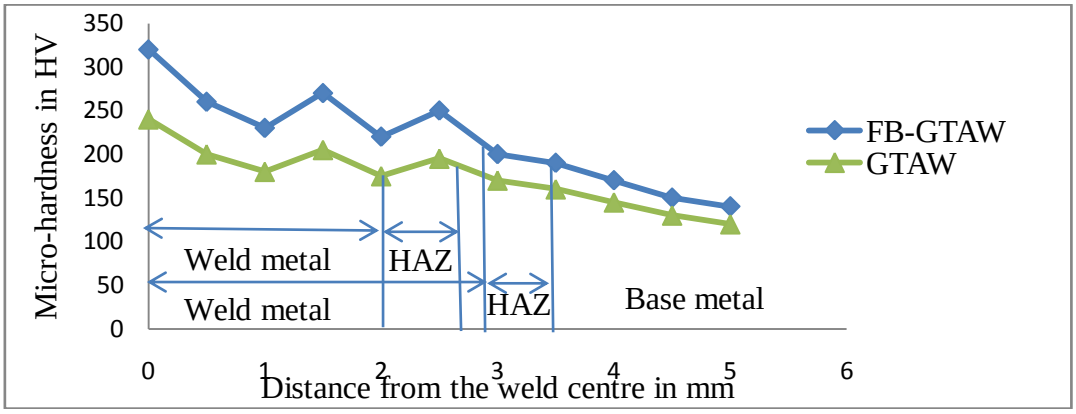


Figure14 Micro-hardness at 120A

### 4.3.2. MICRO HARDNESS AT 140 AMPERE BY FB-GTAW AND GTAW

The micro hardness for FB-GTAW was about 320 HV due to formation of martensite in the weld pool. The hardness decreases with the increase in heat input. This is due to low cooling rate at high heat input. The micro hardness of 240 HV has been observed in the weld metal without using flux. This is due to formation of acicular ferrite and pearlite in the weld metal.

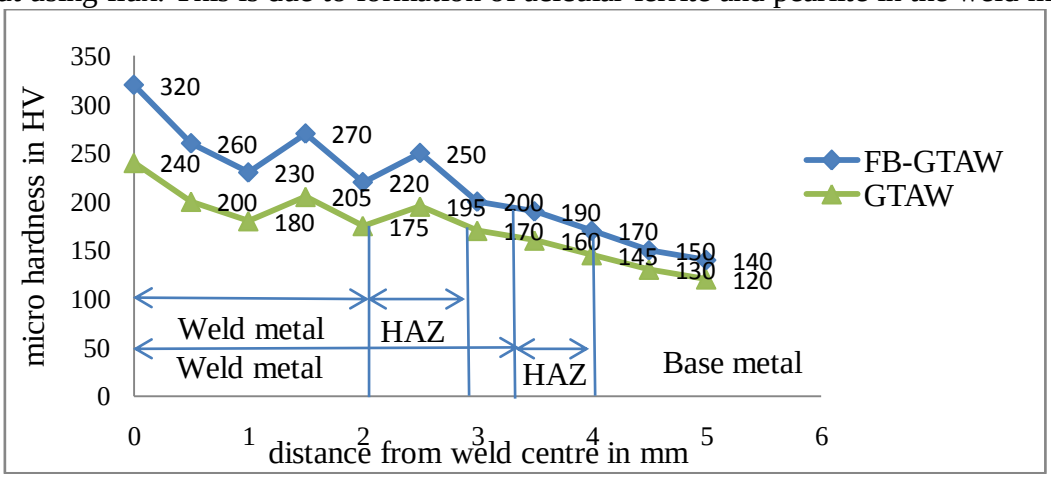


Figure 15 Micro-hardness at 140 A

### 4.3.3. MICRO HARDNESS AT 160 AMPERE BY FB-GTAW AND GTAW

Also, the micro hardness at 160 A by using flux was 300 HV. The cooling rate will further decrease due to increase in the heat input. The micro hardness at 160 A with GTAW process was 220 HV. This is due to low cooling rate which gives coarse microstructure of pearlite.

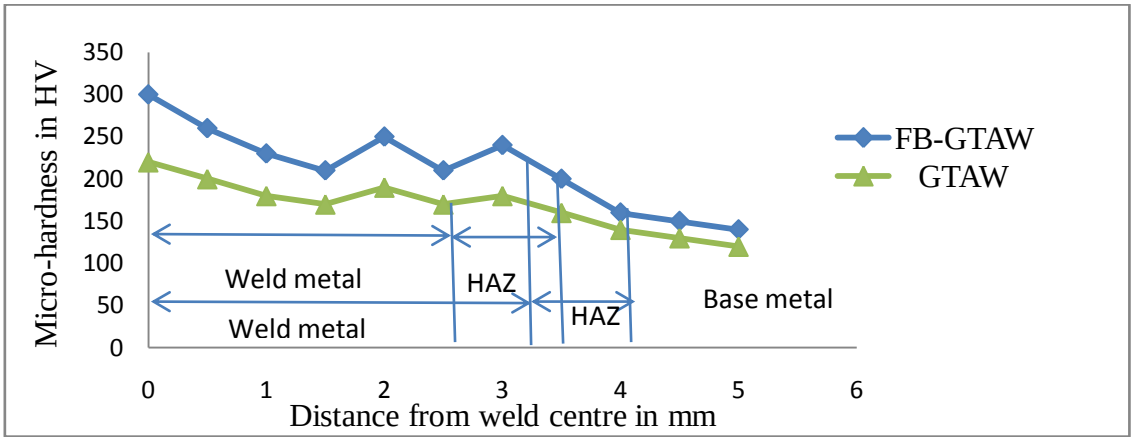


Figure 16 Micro hardness at 160 A

## 4.4. SIMULATION STUDY OF FLUX BONDED GTAW

The cross-sectional view of the bead geometry as simulated by MSc MARC software is calculated. The width and depth of penetration of the bead geometry are calculated and compared with the experimental results.

### 4.4.1. TEMPERATURE PROFILE OF MOVING HEAT SOURCE

The moving heat source gives the temperature value at different locations. At the centre of the weld the temperature is highest and moving away from the centre the temperature decreases and is least at the end of the plate. The temperature contour at different locations gives the temperature values. At this location the highest temperature is approaching $1370^0$C while the lowest temperature is about $25^0$C. The variations of the temperature at different locations as moving outward from the centre are shown. The different colour contour gives the variation in temperature. The maximum temperature is recorded near the centre of the welding arc.

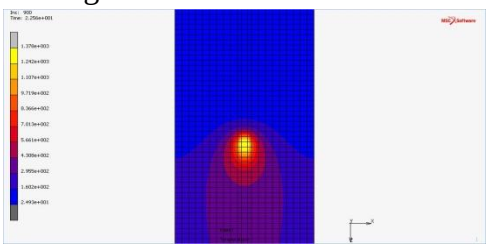

Figure17 Temperature profile at midpoint of the weld

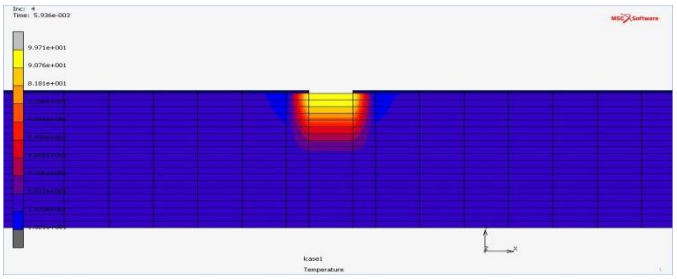

Figure 18 Temperature profile at the start of the weld

## 4.5. CALCULATION OF DEPTH OF PENETRATION AND BEAD WIDTH FOR FB-GTAW PROCESS

The depth of penetration and bead width achieved by using flux layer on the base metal at 120A is shown in Figure 5.24. The depth of penetration is 2.82mm and bead width is 6.12 at 120A. Thus, shape factor is 2.17. Thus, the depth of penetration at 140A for FB-GTAW process is 3.02mm and bead width is 6.54mm. Thus, shape factor is 2.162. The depth of penetration and bead width is shown in Figure 5.26. The depth of penetration is 3.54mm and bead width is 6.24mm. Thus, shape factor is 1.763.

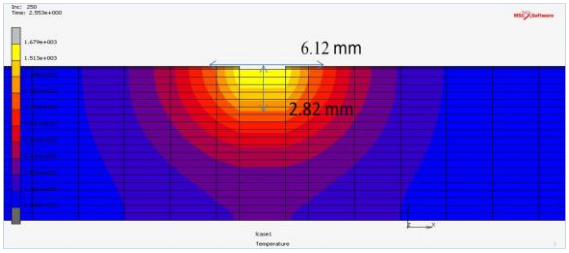


Figure19 Depth of penetration and bead width at 120 A

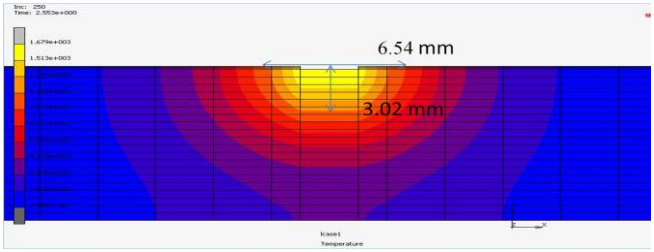


Figure20 Depth of penetration and bead width at 140 A

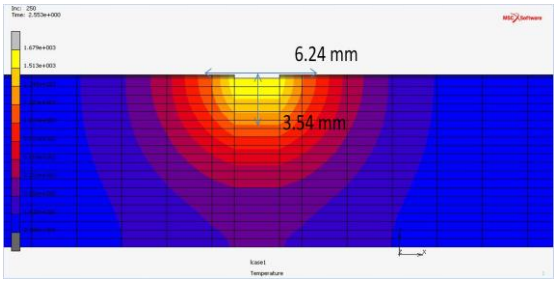


Figure21 Depth of penetration and bead width at 160 A

### 4.6 COMPARISON OF TIME-TEMPERATURE PLOT FOR FLUX BONDED GAS TUNGSTEN ARC WELDING

Simulation results show that the maximum temperature is about 1200°C at 22 seconds. The experimental result shows that the peak temperature was 1175°C at 22 seconds. The cooling was calculated for simulation results and its value was 166.67°C/s and for experimental results its value was 160.22°C/s.

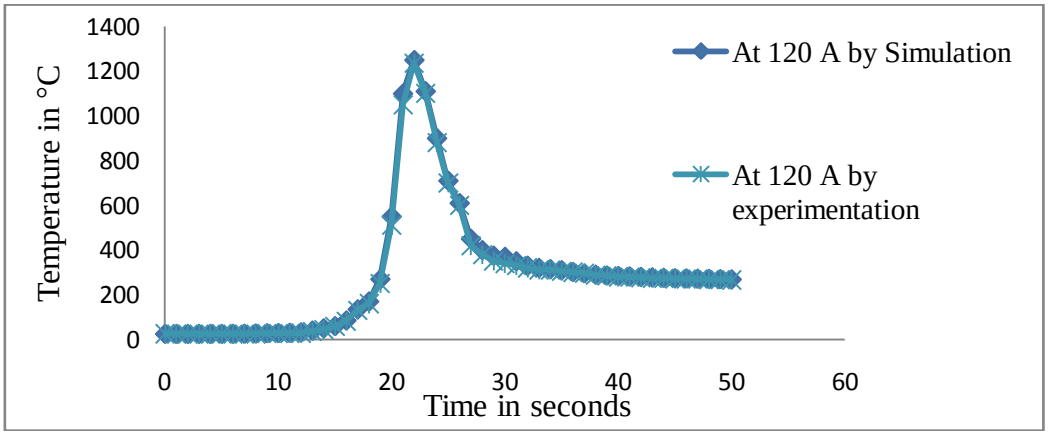


Figure 22 Comparison of Time-Temperature plot for Flux Bonded Gas Tungsten Arc Welding at 120 A

Simulation results show that the maximum temperature is about 1280°C at 22 seconds. The experimental result shows that the peak temperature was 1250°C at 22 seconds. The cooling rate for simulation results was calculated and its value was 142.86°C/s. The cooling rate foe experimental results were calculated and its value was 138.61°C/s.

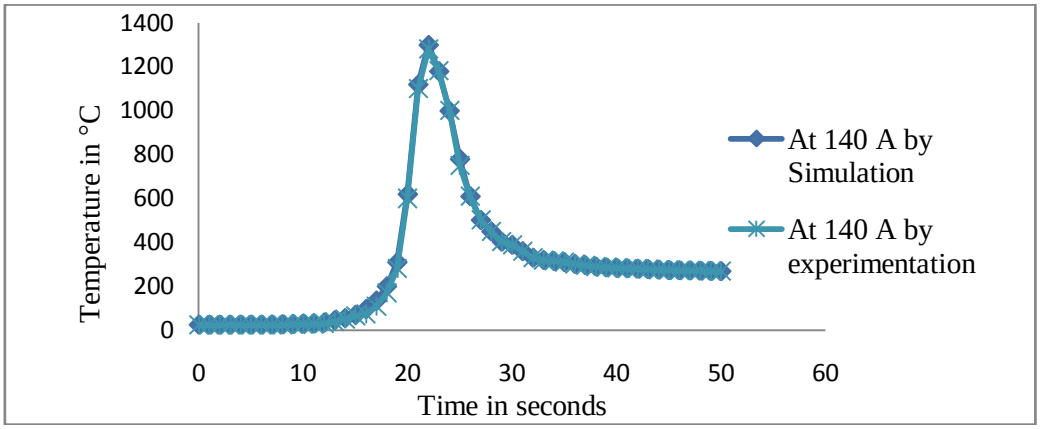


Figure 23 Comparison of Time-Temperature plot for Flux Bonded Gas Tungsten Arc Welding at 140 A

Simulation results show that the maximum temperature is about 1387°C at 22 seconds. The experimental results show that the maximum temperature at 22 seconds is about 1350°C. The cooling rate for FB-GTAW process by simulation was 100.33°C/s and with experimentation were 96.67°C/s.

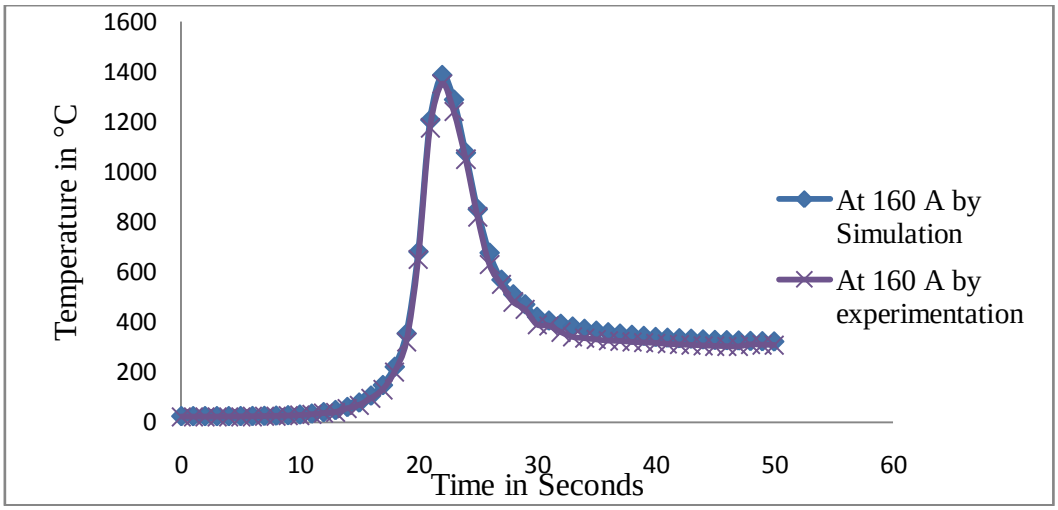


Figure 24 Comparison of Time-Temperature plot for Flux Bonded Gas Tungsten Arc Welding at 160 A

Percentage error is calculated between experimental and simulation Time-Temperature plot for FB-GTAW process. There is difference between the peak temperature and cooling rates obtained in simulation and experimental results.

Table4 Comparison between experimental and simulated peak temperature and cooling rate

| Current (A) | Peak temperature (°C) | | Cooling rate (°C/s) | | % error | |
|---|---|---|---|---|---|---|
| | Simulation | Experimental | Simulation | Experimental | Peak temperature | Cooling rate |
| 120 | 1200 | 1175 | 166.67 | 160.22 | 2.08 | 3.87 |
| 140 | 1280 | 1250 | 142.86 | 132.61 | 2.34 | 2.97 |
| 160 | 1387 | 1350 | 100.33 | 92.67 | 2.67 | 3.65 |

### 4.7.COMPARISON OF SHAPE FACTOR FOR FB-GTAW PROCESS

It is very evident that there is very less difference between simulated and experimental results which is clear from the Table 5. There is maximum error of 0.395 % has been encountered in the experimental and simulated results. Thus, the above study shows us that there is very less error between the two values.

Table 5 Comparison between simulated and experimental results

| Specimen No. | Current Ampere | Heat input (KJ/s) | Bead width (mm) | | Depth of penetration (mm) | | Width to depth ratio (shape factor) | | % error |
|---|---|---|---|---|---|---|---|---|---|
| | | | Exp. | FEM | Exp. | FEM | Exp. | FEM | |
| Sample 1 | 120 | 0.720 | 6.1 | 6.12 | 2.8 | 2.82 | 2.18 | 2.17 | 0.355 |
| Sample 2 | 140 | 0.840 | 6.51 | 6.53 | 3.01 | 3.02 | 2.163 | 2.162 | 0.0462 |
| Sample 3 | 160 | 0.960 | 6.21 | 6.24 | 3.51 | 3.54 | 1.77 | 1.763 | 0.395 |

## 5. CONCLUSIONS

1. Shape factor has been calculated at different heat input i.e. 120 A, 140 A and 160 A. The results show that the shape factor decreases with the increase in the current value or heat value significantly.
2. The shape factor has been calculated for FB-GTAW process and compared with normal GTAW process. The results show that the shape factor decreases in FB-GTAW process as compared to normal GTAW process.
3. The shape factor at 120 A has been decreased by 29.22% with FB-GTAW process. The shape factor decreased by 19.59% at 140 A with FB-GTAW process and shape factor was decreased by 31.13% at 160 A with FB-GTAW process.
4. The depth of penetration has been increased and bead width has been constricted by with FB-GTAW process as compared with normal GTAW process. it was found that when the amount of surface-active element is between 70-200 ppm then the direction of metal flow changes from outward to inward this was due to change in surface temperature gradient at the periphery of weld pool from negative to positive. This happens due to flow of metal in reverse direction from outward to inward (Reverse Marangoni effect).
5. The depth of penetration has been increased by 38.6% at 120 A with FB-GTAW process. The depth of penetration has been increased by 23.89% at 140 A with FB-GTAW process and depth of penetration was increased by 43.26% at 160 A with FB-GTAW process.
6. Micro-structure has been observed in the weld metal with FB-GTAW process and normal GTAW process at three different currents i.e., 120 A, 140 A and 160 A. It has been observed that the martensite formation takes place in the weld metal with FB-GTAW process. The peak temperature in the weld metal at 160 A was 1350°C and cooling rate was 96.67 °C/s The pearlite and acicular ferrite was observed in the weld metal in normal GTAW process. This is because the peak temperature reached was less and there is no austenite formation.
7. Micro-hardness has been observed for all current values i.e., 120 A, 140 A and 160 A. It has been observed that the Micro-hardness decreases with increasing current. This is due

to the decrease in the cooling rate with increasing current value. The cooling rate at 120 A was 160.22°C/s, at 140 A was 138.61°C/s and at 160 A was 96.67°C/s. There will be decrease in the ferrite content as well as lower martensite formation in the weld pool as the current value increases due to slower cooling rate.

8. The Micro-hardness at 120 A with FB-GTAW process at weld centre was 350 HV and with normal GTAW process was 260 HV. The Micro-hardness at 140 A with FB-GTAW process at weld centre was 320 HV and with normal GTAW process was 240 HV. Also the Micro-hardness at 160 A with FB-GTAW process at weld centre was 300 HV and with normal GTAW process was 220 HV. This is due to formation of martensite in the weld metal with FB-GTAW process as compared to GTAW process.
9. A model has been developed on Marc (NASTRAN) to predict effect of flux on Shape factor for GTAW process and results predicted by model compared with experimental data and error was calculated.
10. The error of 0.355% has been calculated for shape factor at 120 A, 0.0462% at 140 A and 0.395% at 160 A. Thus, a maximum of 0.395 % error calculated for FB-GTAW process at 160 A which is within acceptable limits.
11. Model also predicts temperature distribution during welding process and results are compared with experimental time temperature data and results are satisfactory.
12. It has been found that time temperature data has variation at its peak temperature.The error calculated at 120 A for FB-GTAW process is 2.08 %, 2.34 % at 140 A and 2.67 % at 160 A and found to be satisfactory.
13. The cooling rates have variation between simulated and experimental results. Thus error calculated is 3.81 % at 120 A, 2.97 % at 140 A and 3.65 % at 160 A and found to be within satisfactory limits.

## 6. ACKNOWLEDGMENT

The above research work is done at Sant Longowal Institute of Engineering Technology. We are grateful to all faculty members of the Mechanical Engineering Department forguiding me at correct time so that I can have a touch at final destination. We are also thankful to the technicians of Departmental workshops who constantly tried to enhance the value of this work from time totime.

## REFERENCES

1. Shrivas S. P., Vaidya S. K., Khandelwal A. K., & Vishvakarma A. K. (2020), “Investigation of TIG welding parameters to improve strength”, Journal of Materials Today: Proceedings, 26, pp. 1897-1902.
2. Kou S. (2003), Welding metallurgy, New Jersey, USA, 431(446), pp. 223-225.
3. Jayakrishnan S., & Chakravarthy P. (2017), “Flux bounded tungsten inert gas welding for enhanced weld performance—A review”, Journal of Manufacturing Processes, 28, pp. 116-130.
4. Modenesi P. J., Apolinario E. R. & Pereira I. M. (2000), “TIG welding with single-component fluxes”, Journal of materials processing technology, 99(1-3), pp. 260-265.
5. Aniruddh S. Negi (2017), “Finite element analysis of multi-pass shielded metal arc welding process to predict temperature distribution and residual stress in SS-304 weldment”, M.Tech Thesis, SLIET Longowal, pp. 26-37.
6. Rückert, G., Huneau B. & Marya S. (2007), “Optimizing the design of silica coating for productivity gains during the TIG welding of 304L stainless steel”, Journal of Materials & design, 28(9), pp. 2387-2393.

**7.** Kala S. R., Prasad N. S. & Phanikumar G. (2014), "Studies on multipass welding with trailing heat sink considering phase transformation", Journal of Materials Processing Technology, 214(6), pp. 1228-1235.
**8.** Tseng K. H. & Shiu Y. J. (2015), "Effect of thermal stability of powdered oxide on joint penetration and metallurgical feature of AISI 4130 steel TIG weldment", Journal of Powder Technology, 286, pp. 31-38.
**9.** Singh A. K., Dey V. & Rai R. N. (2017), "Techniques to improve weld penetration in TIG welding (A review)", Journal of Materials Today: Proceedings, 4(2), pp. 1252-1259.
**10.** Kumar K., Deheri S. C. & Masanta M. (2019), "Effect of activated flux on TIG welding of 304 austenitic stainless steel", Materials Today: Proceedings, 18, pp. 4792-4798.
**11.** Vidyarthy R. S. & Sivateja P. (2020), "Influence of activating flux tungsten inert gas welding on mechanical and metallurgical properties of the mild steel", Journal of Materials Today: Proceedings, 28, pp. 977-981.
**12.** Unni A. K. & Vasudevan M. (2020), "Numerical modelling of fluid flow and weld penetration in activated TIG welding", Materials Today: Proceedings, 27, pp. 2768-2773.